New phase change nanomaterial for solar use: synthesis and characterization

L Maifi[1]*, K Agroui[1], O Hioual[2], A Chari[3] and T Karbache[3]

1. Research Center in Semiconductors Technology for Energetic (CRTSE) Algiers, Algeria
2. Mathematics and Computer Science Department Abbes Laghrour, University Khenchela, Algeria
3. Physical Chemistry of Semi-Conductor Laboratory, University of Constantine1, Algeria

ABSTRACT

In this paper, we used a commercial paraffin type ($C_{25}H_{52}$) which was doped with TiO_2, $ALCL_3$ and AL_2O_3 in the range of 0 and 20% by mass and atom. The monitoring of the temperature over time was measured during the descent of 150°C to ambient. For all dopants, the phase change time, thermal conductivity, latent heat and specific heat increase with the doping rate and the mass of the paraffin. The experimental results show that the phase change time, thermal conductivity, latent heat and specific heat are more important in the case of doping with $ALCL_3$ compared to the other two dopants.

1. INTRODUCTION

One of the solutions to the problem of low thermal-electric efficiency of the solar panel is the hybrid system design allowing the simultaneous production of thermal energy and electricity. To do this, we must imagine devices that allow the recovery of thermal energy by cooling the solar panel. The gain is then double, because we improve the efficiency of the panel by cooling, and we recover the usable thermal energy. For this purpose, the use of phase change materials (paraffin) allows the recovery of thermal energy during the phase change cooling the panel, which improves performance. Several works are carried out, on the cooling of the cells and the storage of heat in a phase change material, either by improving the cooling behind the panels thanks to natural, or forced convection, or by the absorption of the excess heat from the panels [1-4]. One of the objectives of using innovative phase change materials is to extend the cooling time of the panels beyond 8 hours, which corresponds to the average time of strong sunshine in our Saharan regions. Unfortunately, phase change materials (paraffin) have a fairly low thermal conductivity of the order $0.2 \ Wm^{-1}K^{-1}$ on average, which does not allow good heat transfer during cooling/heating processes [1-8].

To solve this problem during each process, the injection of very fine solid particles of high thermal conductivity into the phase change material is proposed [5-7].

---
*Corresponding Author: maifi.lyes@crtse.dz

2. RELATED WORK

Several works are carried out, on the cooling of the cells and the storage of heat in a phase change material, either by improving the cooling behind the panels thanks to natural or forced convection, or by the absorption of the excess heat from the panels.

In the work of Ho and Gao [9] a phase change material embedded by nanoparticles was prepared by adding nanoparticles of alumina (Al_2O_3) in paraffin (n-octadecane) by means of a surfactant non-ionic. Paraffin Nanoparticle Mixtures (NEPCM) contain 5% and 10% nanoparticles, respectively. Their effective thermos-physical properties, latent heat of fusion, density, dynamic viscosity, and thermal conductivity, have been investigated experimentally. The density of the paraffin/nanoparticle mixture measured agrees perfectly with that predicted on the basis of mixing theory. The measured thermal conductivity and dynamic viscosity of the paraffin / nanoparticle mixture show a non-linear variation as a function of temperature.

Khodadadi and Hosseinizadehont [10] improved performance of phase change materials (PCM) through the dispersion of nanoparticles. Nanoparticle-enhanced phase change materials exhibit high thermal conductivity compared to base PCM. The problem is to study the solidification in a differentially heated square cavity that contains a nanoparticle (water, plus copper nanoparticles), Due to the increase in thermal conductivity and, also the decrease of the fusion latent heat.

Wu et al [11] investigated the potential of Al_2O_3-H_2O nanofluids as a new phase change material for thermal energy storage in cooling systems. The thermal response shows that the addition of Al_2O_3 nanoparticles remarkably decreases the degree of super cooled water, advances the freezing start time and reduces the total freezing time. They showed that by adding only 0.2% by weight of Al_2O_3 nanoparticles, the total freezing time of Al_2O_3-H_2O nanofluids can be reduced by 20.5%.

Qinbo et al [12] have developed improved phase change material mixture paraffin / nanoparticles, by the suspension of a small amount of the nanoparticles of TiO_2 in a saturated aqueous solution of $BaCl_2$. The thermal conductivity, the degree of sub cooling, the latent heat, the specific heat, and the rheological behaviors of paraffin / nanoparticle mixture were studied. The experimental results show that with a volume fraction of 1.13%, the thermal conductivity of paraffin / nanoparticle mixture is increased by 12.76% at 5°C, the degree is reduced by 84.92%. Latent heat is reduced. The thermal conductivity increases with the increase in volume fraction, which has no effect on the storage system.

In this work, we are interested in the evolution of the phase change time, thermal conductivity and latent heat as a function of the mass of a commercial paraffin type $C_{25}H_{52}$. Another study concerns its evolutions according to the nature of the dopant and the doping rate. This manages that it is of great importance in cooling solar panels in Saharan environments using thermal energy storage involving latent heat in a phase transformation material. for the thermal characterization we do the Differential scanning calorimetry and Thermogravimetric Analysis and for the optical analysis we do the FTIR and observation bar SEM.

3. EXPERIMENTAL IMPLEMENTATION

In this work, we used a commercial paraffin type $C_{25}H_{52}$ as phase change material which was doped with TiO_2, $ALCL_3$ and AL_2O_3 with a doping rate of 0, 8, 14 and 20%. The paraffin was heated up to 150°C to have its liquid phase using a STUART CC62 heater equipped with a STUART SCT1 regulator allowing the temperature to be measured as a function of time. We also used masses of 5g, 10g, 20g and 30g of paraffin. The dopants used are TiO_2 brand RIEDEL DE HAEM, pure $ALCL_3$ hexahydrate type RIEDEL DE HAEM and AL_2O_3 powder brand PRESI. Temperature monitoring over time was measured during the descent from 1500°C to ambient. For a mass "m" of paraffin, we calculated the mass "m_0" of the dopant so that the ratio gives the mass and atomic percentage of the dopant. (See Figure 1, and Table 1).

$$\text{chemical formula } C_{25}H_{52}: \qquad C_{25}H_{52} + 38O_2 \rightarrow 25CO_2 + 26H_2O \tag{1}$$
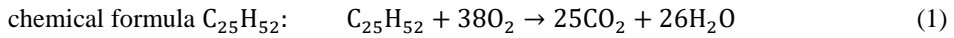
C: Carbon, H: hydrogen and O: oxygen
CO_2: Carbon dioxide and H_2O: The water

Figure 1: Dopants used

Table 1: The properties of dopants and paraffin used

	Density g.cm^{-3}	Fusion Temperature °C	Molar mass g.mol^{-1}	Boiling Temperature °C
TiO_2	3.9-4.3 g.cm^{-3}	1650-1855°C	79.90 g.mol^{-1}	2500-3000°C
$ALCL_3$	2.44-2.48 g.cm^{-3}	190°C à 2.5 atm	133.3 g.mol^{-1}	182.7°C à 752 mmHg
AL_2O_3	3.97 g.cm^{-3}	2050°C	102 g.mol^{-1}	2980°C
Paraffin	0.9 g.cm^{-3}	50-59°C	404 g.mol^{-1}	190°C

4. RESULTS AND DISCUSSION

Tables 2, 3, 4 and 5 show the phase change time of paraffin doped with TiO_2, $ALCL_3$ and AL_2O_3 for different doping rate 'x'. It can be seen that this phase change time increases with the doping rate regardless of the type of dopant. However, as shown in Tables 2, 3, 4 and 5, the phase change time is better for $ALCL_3$ and this whatever the doping. The phase change time decreases going from $ALCL_3$ to AL_2O_3 then to TiO_2.

Table 2: Phase change time for three dopants and different doping rates for a mass of 5g

Dopant	TiO_2	$ALCL_3$	AL_2O_3
Phase change time (s) 0%	380.96	380.96	380.96
Phase change time (s) 8%	414.185	580.215	421.886
Phase change time (s) 14%	520.321	644.259	532.214
Phase change time (s) 20%	645.59	746.667	6664.667

Table 3: Phase change time for three dopants and different doping rates for a mass of 10g

Dopant	TiO_2	$ALCL_3$	AL_2O_3
Phase change time (s) 0%	482.917	482.917	482.917
Phase change time (s) 8%	536.521	914.042	656.755
Phase change time (s) 14%	661.302	1103.23	773.57
Phase change time (s) 20%	773.542	1230	863.812

Table 4: Phase change time for three dopants and different doping rates for a mass of 20g

Dopant	TiO_2	$ALCL_3$	AL_2O_3
Phase change time (s) 0%	1002.936	1002.936	1002.936
Phase change time (s) 8%	1287.027	1811.19	1533.254
Phase change time (s) 14%	1463.374	1997.931	1800.321
Phase change time (s) 20%	1697.871	2160	1905.524

Table 5: Phase change time for three dopants and different doping rates for a mass of 30g

Dopant	TiO_2	$ALCL_3$	AL_2O_3
Phase change time (s) 0%	1868.469	1868.469	1868.469
Phase change time (s) 8%	2208.91	2834	2594
Phase change time (s) 14%	2504.81	3506	2880
Phase change time (s) 20%	2760	4035	3120

4.1. Evolution of fusion time as a function of the doping rate and the mass of paraffin

Figures 2 and 3 show the evolution of the phase change time as a function of the paraffin mass for three types of dopants and as a function of different doping rates.
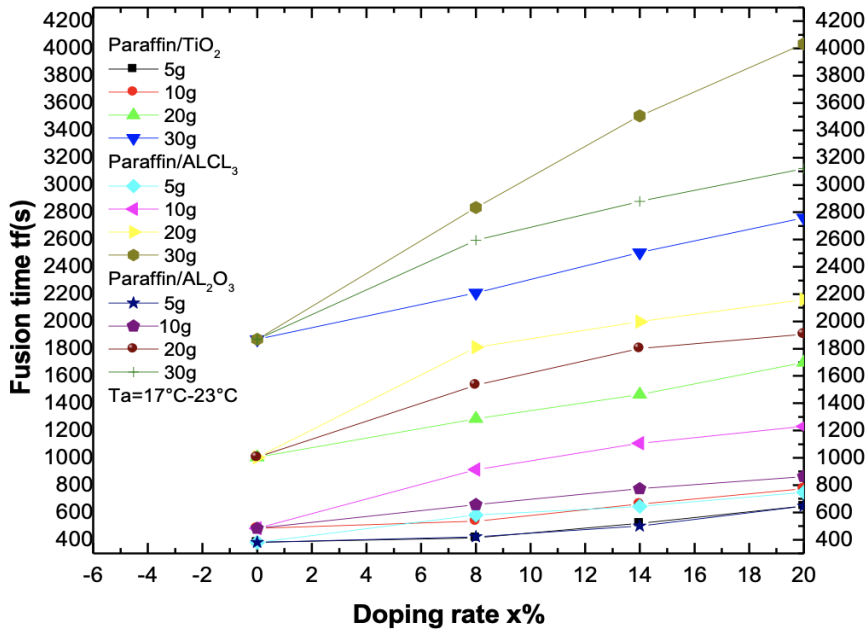

Figure 2: The evolution of the phase change time as a function of different doping rates for the three types of dopants

The observation of Figures 2 and 3 confirms that the phase change time increases with mass, for all doping rates. For a given mass, this time increases as a function of the doping rate and the evolution is much better for $ALCL_3$ compared to AL_2O_3 and TiO_2. Regarding doping, the evolution of phase transformation time as a function of "x" doping rate can be explained by using the latent heat of fusion of paraffin. The latter increases as a function of the doping rate, which increases the heat to be evacuated during a phase change, which lengthens the phase change time, the temperature measurement system as a function of time always being the same.

In addition, the phase change time enters into the characterization of the heat transfer between the paraffin and the ambient air through the surface of the glass. This transfer is proportional to the specific heat (C_p) of the paraffin. As the phase change time increases, indicating that the amount of heat transferred is more important especially as the doping level is high. Clearly this indicates that the specific heat of the paraffin increases with the rate of doping.
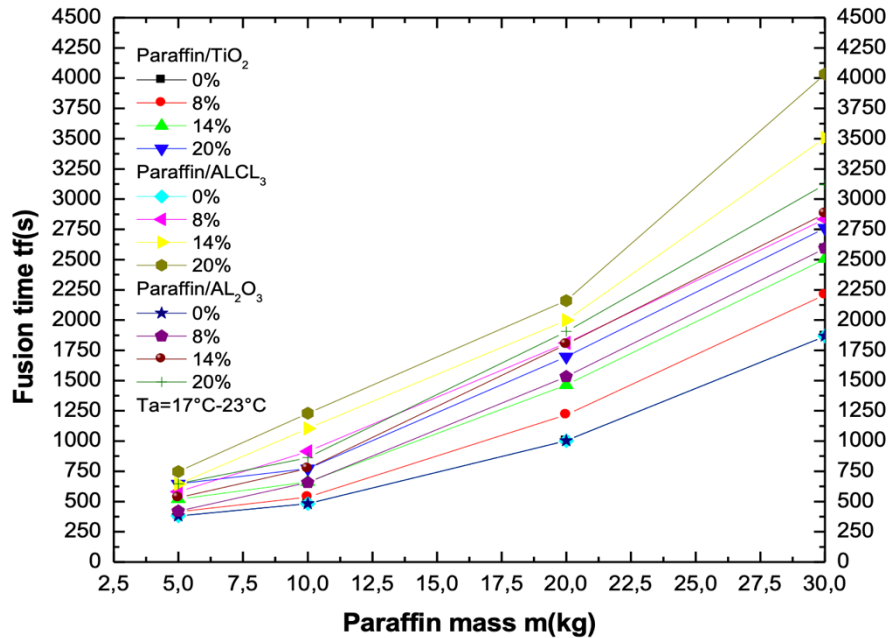
Figure 3: The evolution of the phase change time as a function of the paraffin mass for the three types of dopants

4.2 DSC Differential scanning calorimetry measurement results:

In our study, the sample undergoing an endothermic transition (transition from solid phase to liquid phase) will need more heat to maintain the same temperature as the reference, because it absorbs energy in the case of fusion. The measurements are carried out with a pierced crucible lid and under nitrogen purging, the temperature rise measurement is carried out from zero temperature 0°C to the temperature envisaged in our study equal to 100°C, And a speed of 5°C/min.

The Figure 4 shows the changes in heat flow of the phase change, commercial and doped paraffin material as a function of furnace temperature. The main peak shows the solid-liquid phase change. We note that there is no change in heat flow between sample and vacuum until the temperature of the start of the phase change (45°C, 8.1 J/g), where the material begins to absorb the heat and heat absorbed is maximum then returns to zero point when it completely turns into liquid.

From the curves, we can deduce:

The heat absorbed by the materials increases with increasing doping rates for all types of dopants. The heat absorbed by the material is very important for $ALCL_3$:

- 194.28 J/g for commercial paraffin,
- 264.97 J/g for paraffin doped 14% AL_2O_3,
- 392.14 J/g for paraffin doped 14% $ALCL_3$.

There is a relationship between thermal conductivity and specific heat and latent heat when we increase thermal conductivity with injection of nanoparticles, latent heat increases and increases phase change time, this study confirms results get on the phase change time calculation.

It can be seen from Table 6 and Figure 4 that the solid-liquid phase change (fusion temperature) temperatures of MCPs composites are close to those of commercial paraffin and an improvement is made with the addition of the oxides. This means that there is no chemical reaction between the powders and the paraffin. This is confirmed by the results of the FTIR analysis [11].
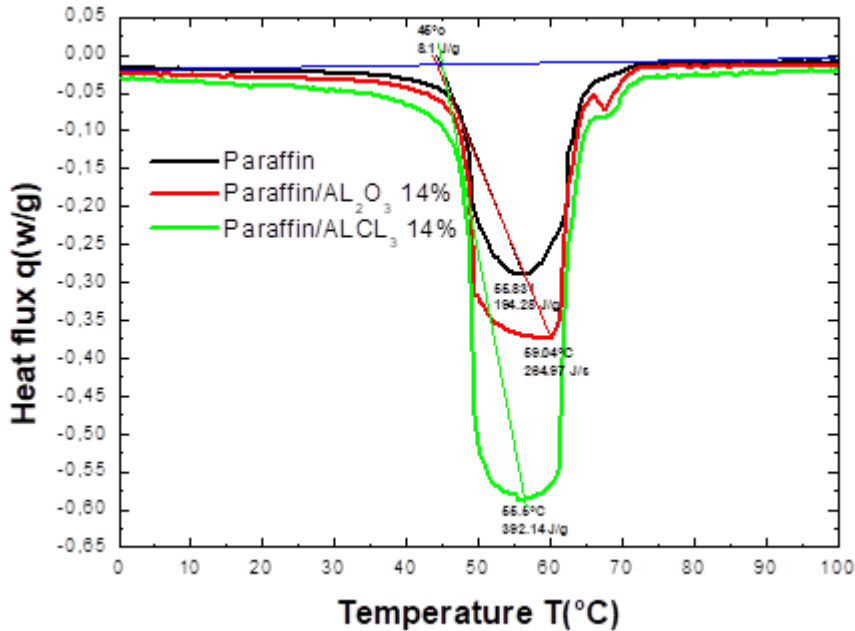

Figure 4: DSC curves q = f(T) of pure paraffin, doped with 14% AL_2O_3 and 14% $ALCL_3$.

Table 6: DSC of paraffin [11]

	Solid-liquid fusion endothermic transition			
Temperature	T_f °C	T_p °C	T_e °C	Latent heat J/g
Paraffin	52.68	57.03	59.69	154.87

4.3 Thermogravimetric Analysis (TGA)

TGA is a technique for measuring the loss of mass of a substance undergoing a temperature regime in a controlled atmosphere. This temperature regime automatically can be at $T = T_0$ and we measure dm = f(t) or at $T = T_0 + kt$ and we measure dm = f(T) or dm = f(t). The heating of the substance causes its degradation (transformation) with gain or loss of mass which is measured according to whether the substance loses or gains volatile constituents. The results given by the measured loss of mass for pure paraffin doped with TiO_2, AL_2O_3 and $ALCL_3$ are present in Figure 5.
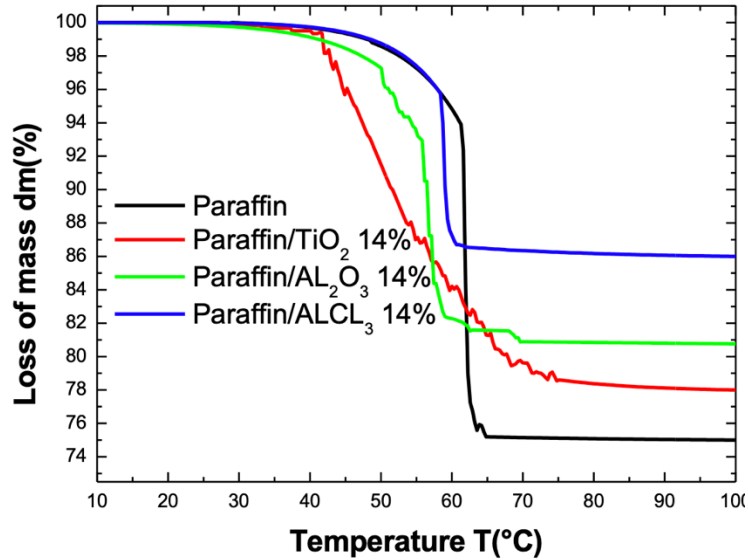
Figure 5: The loss of mass 'dm' as a function of temperature for paraffin pure, paraffin doped with TiO_2, AL_2O_3 and $ALCL_3$ (14%).

Normally the fusion or the change of structure is indictable by ATG (no loss or gain of mass). In our case, we can observe a loss of mass that can be observed in the air bubbles in the paraffin which vaporizes on heating. Curve 5 shows that whatever the dopant, the doping rate improves the preservation of paraffin. It is important to note that the improvement is better for paraffin doped with $ALCL_3$ or the mass loss is 12% while it is 18%, 22% and 26% for paraffin doped with AL_2O_3, TiO_2, and commercial paraffin respectively. What he does relate is that doping with $ALCL_3$ improves thermal conductivity, latent heat as well as the phase change time of the substance.

4.4 Evolution of the thermal conductivity of fusion as a function of the doping rate and the nature of the dopant

The principle of the test bench for determining thermal conductivity consists of imposing a temperature difference between the faces of the composite in contact with the flowmeters until a heat flow is observed at zero (equilibrium state). The thermal conductivities are then calculated by the following expression [11]:

$$\lambda = \frac{e.\Sigma\,\phi}{2.\Delta T} \tag{2}$$

where λ and e are the thermal conductivity and the material thickness respectively, Φ is the heat flux and T is the material temperature.

The obtained results by the simulation of the model program JAVA Model of Yu, after the calculations of temperatures as a function of time given, by the program and the DSC. (See Figures 6,7 and 8).

The measured thermal conductivity of commercial paraffin shows a non-linear variation with temperature. The simulation results calculated by the experimental data show that with a volume fraction of 0%, 8%, 14% and 20% thermal conductivity increases in the solid phase and decreases in the solid-liquid and liquid phase. Thermal conductivity increases with increasing doping rate and is better for ALCL$_3$. Nanoparticle doped phase change materials exhibit high thermal conductivity compared to the base material.
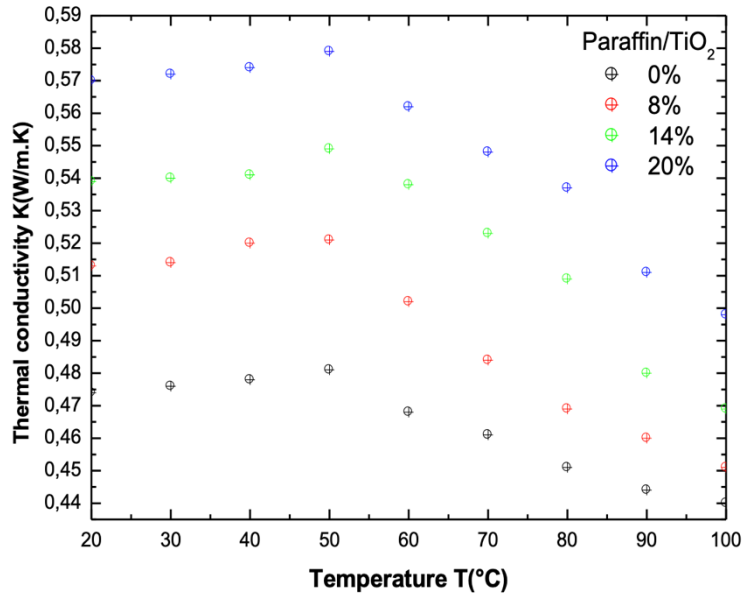
Figure 6: The evolution of thermal conductivity as a function of paraffin doped TiO$_2$ temperature.
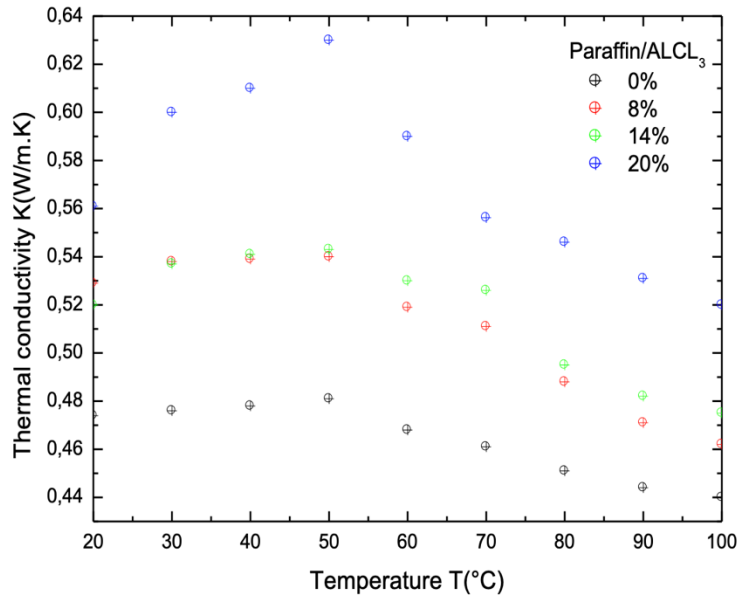

Figure 7: The change in thermal conductivity as a function of paraffin doped ALCL$_3$ temperature.
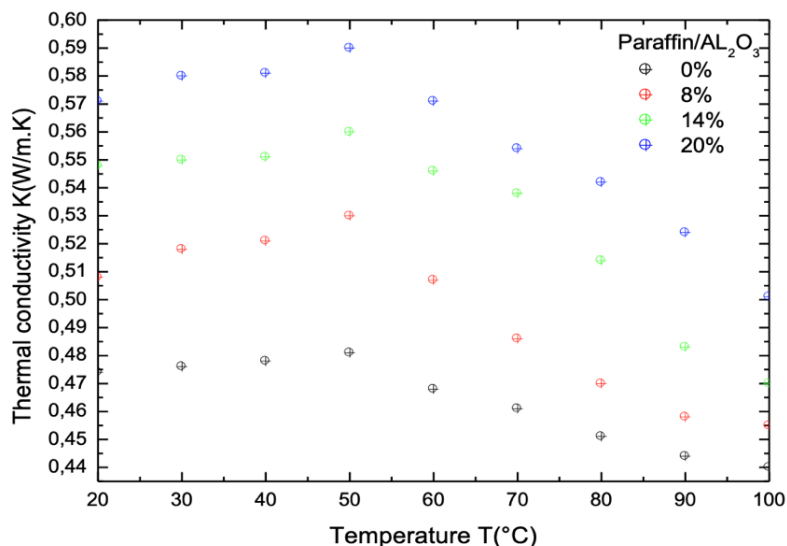
Figure 8: The change in thermal conductivity as a function of paraffin doped AL_2O_3 temperature

4.5 Fourier infrared spectrometry (FTIR) analysis

Infrared IR absorption spectroscopy is a most widely used technique for the characterization of organic and inorganic compounds in laboratories. It is a rapid characterization method that is sensitive to most of the existing molecules.

The main peaks observed on the infrared spectrum of our paraffin layer, paraffin doped with 14 and 20% TiO_2 oxide, $ALCL_3$ and AL_2O_3 are shown in Figures 9, 10.
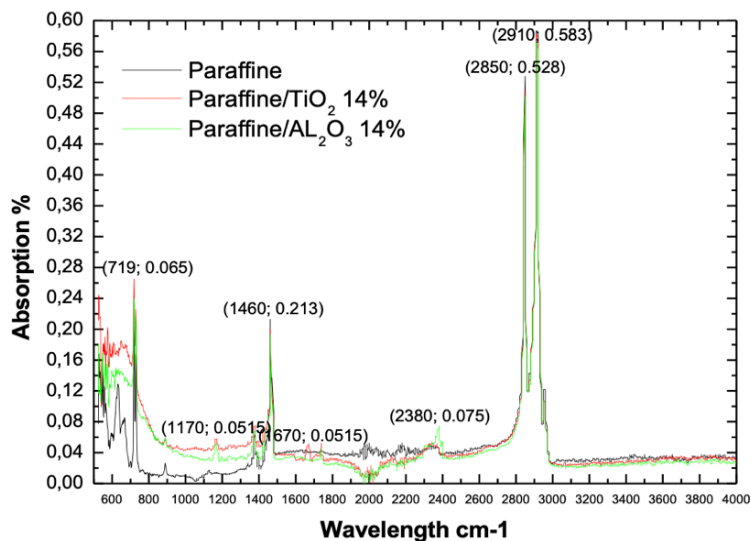

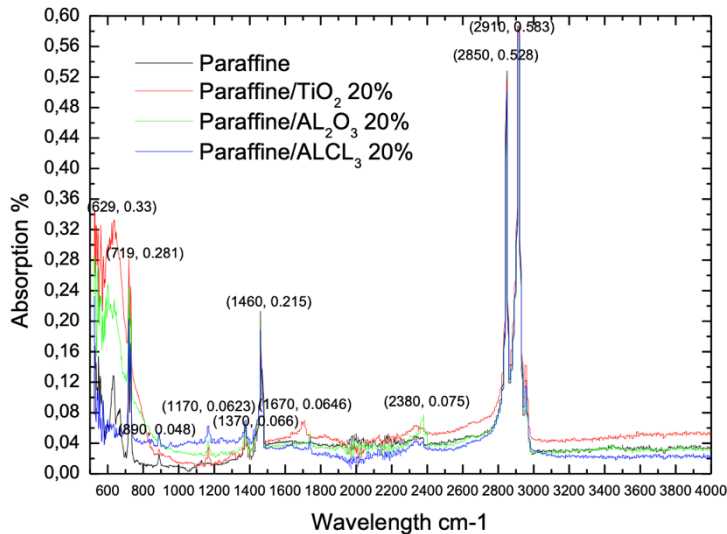Figure 9: FTIR pure paraffin, paraffin doped TiO_2 14% and AL_2O_3 14%

Figure 10: Paraffin FTIR doped with 20% TiO_2, AL_2O_3 and $ALCL_3$ dopants

The IR absorption peaks of paraffin powder layers located in the range 500 to 4000 cm-1 are those typically encountered for paraffin in the literature [12-16], and which are as follows:

- The peak at 2910 cm^{-1} and 2850 cm^{-1} are due to the vibrations of the C-H bond in the CH, CH_2 and CH_3 groups.
- The peak 1460 cm^{-1} is the strain peak of CH2.
- The 1370 cm^{-1} peak represents the deformations in the plane of C-H and C-C.
- The peak at 2380 cm^{-1} is characteristic of the a-AL_2O_3 bond.
- The peak at 1670 cm^{-1} is characteristic of the TiO_2 bond.
- The band centered at 500-700 cm^{-1} corresponds to the vibrations in stretching mode of the bonds.
- The peak located at 719 cm^{-1} is characteristic of the AL-O-AL bond, and also corresponds to the tilting and deformation vibration out of the plane of the paraffin compounds [8].
- The peak located at 1170 cm^{-1} is the C-O vibrations of ethers and alcohols [13-16].

Comparing the spectra of Figures 9 and 10, it is clear that the FTIR spectrum commercial paraffin, paraffin doped TiO_2 14%, AL_2O_3 14%, TiO2 20%, AL_2O 20% and $ALCL_3$ 20% consists of all the peaks of the paraffin and of the AL and Ti. There is no appearance of new peaks, which thus confirms the absence of chemical reaction between paraffin, TiO_2, $ALCL_3$ and AL_2O_3 [13-16]. We notice in the curves that there are two regions, the first lies between 750 to 4000 which represent the shape of commercial paraffin and doped paraffin they are the same in all graphs and as for the second region, which interests us, it changes from sample to sample and from one doping rate to another. Where we notice that the absorbance increases significantly when we increase the oxide doping rate in the material and that it reaches 32% for (TiO_2, 20%).

We also note that the absorbance is greater in the doping rate of TiO_2 compared to other oxides $ALCL_3$ and AL_2O_3. The results show that our samples do indeed contain C-H groups, characteristic of paraffin, from the wave numbers of 2910 cm-1, 2850 cm-1, 1470 cm-1 and 719 cm-1 [13- 16].

4.6 Observation by SEM scanning electron microscopy

The morphology of the deposited paraffin layer was observed by scanning electron microscopy of our paraffin layer, paraffin doped with 14% TiO_2 oxide deposited on glass by sol-gel technique are shown in Figures 11 and 12.
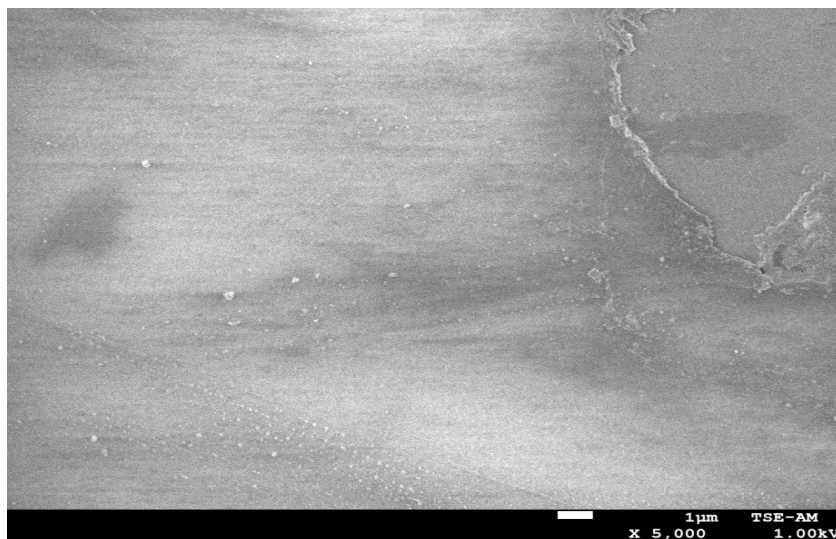

Figure 11: Image of SEM Paraffin doped 14% TiO_2* 5000

In Figures 11 and 12 an SEM photo of a paraffin doped with 14% TiO_2 with a magnification of 5000 and 10000 respectively, we can see that the powder has a homogeneous particle size. The grains have a size of 0.01 nm and less. At higher magnification 10,000 it appears in addition to paraffin grains of titanium oxide of size 0.01nm [17-22]. According to these Figures the morphology of our layer is uniform, homogeneous and compact with the presence of some irregularities. Nevertheless, very little irregularity (non-homogeneity) was detected on our deposits, probably due to some physicochemical criteria (reactivity of the precursor, reaction mechanism, condensation, speed of the deposit, viscosity of the gel, etc.) which governs the final structure of the filing Figure 13 [17-24].

Or, we can also say that: the microstructure of the films is controlled by the physicochemical parameters which are linked to the sol-gel solution (concentration, addition of surfactant, nature of the solvents), the parameters which depend on the forming process (rate of withdrawal), and finally to heat treatments.

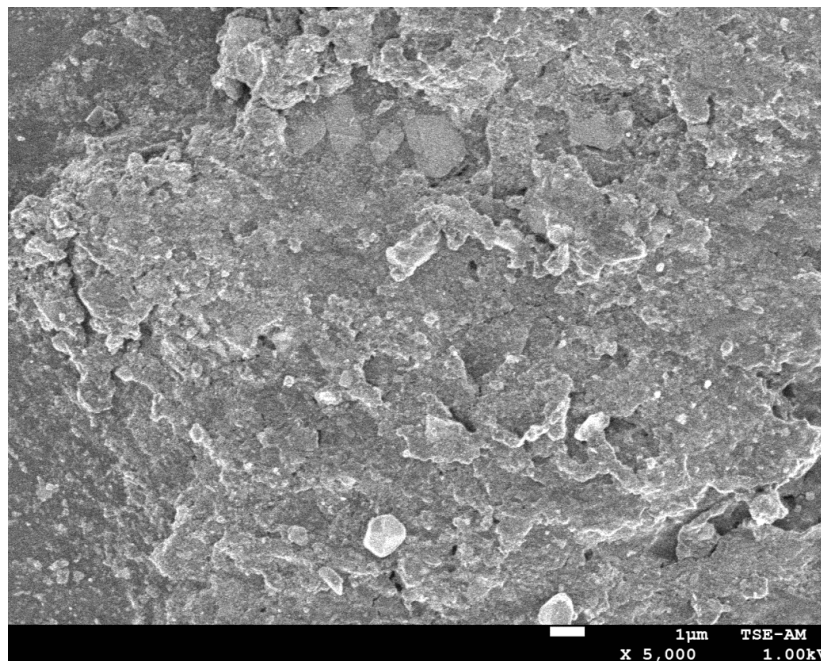Figure 12: Image of SEM Paraffin doped 14% TiO_2 * 10000

Figure 13: Image of SEM Paraffin doped 14% TiO_2 * 5000

5. CONCLUSION

In this work we have seen that the use of phase change materials is an interesting solution for storing energy and cooling photovoltaic modules. The performance of these materials can be improved by the injection of nanoparticles of high thermal conductivity. As a type of dopant, we are interested in the effect of TiO_2, $ALCL_3$ and AL_2O_3 doping of commercial paraffin on the phase change time. For all dopants, the phase change time, thermal conductivity, latent heat and specific heat increase with the doping rate and the mass of the paraffin. The experimental results show that the phase change time, thermal conductivity, latent heat and specific heat are more important in the case of doping with $ALCL_3$ compared to the other two dopants. The results show that our samples do indeed contain C-H groups, paraffin characteristics, from the wave numbers of 2910 cm^{-1}, 2850 cm^{-1}, 1470 cm^{-1} and 719 cm^{-1}. No new peaks appear which thus confirms the absence of a chemical reaction between paraffin, TiO_2, $ALCL_3$ and AL_2O_3.

REFERENCES

[1] F.L. Tan, Constrained and unconstrained melting inside a sphere, Int. Commun. Heat Mass Transfer 35 (2008) 466–475.

[2] F.L. Tan, S.F. Hosseinizadeh, J.M. Khodadadi, L. Fan, Experimental and computational study of constrained melting of phase change materials (PCM) inside a spherical capsule, Int. J. Heat Mass Transfer 52 (2009) 3464–3472.

[3] E. Assis, G. Ziskind, R. Letan, Numerical and Experimental Study of Solidification in a Spherical Shell, Journal of Heat Transfer, Vol. 131, 2009.

[4] Felix Regin, S.C. Solanki, J.S. Saini, An analysis of a packed bed latent heat thermal energy storage system using PCM capsules: Numerical investigation, Renewable Energy 34 (2009) 1765–1773.

[5] Nallusamy N, Velraj R. Numerical and experimental investigation on a combined sensible and latent heat storage unit integrated with solar water heating system. J Sol Energy Eng 2009;131:1–8.

[6] L. Yang, X.S. Zhang, Performance of a new packed bed using stratified phase change capsules, International Journal of Low-Carbon Technology 7 (3) (2021) 208–214.

[7] B.Shobo, A. Mawire, Numerical investigation of a packed bed thermal energy storage system for solar cooking using encapsulated phase change material, Third Southern African Solar Energy Conference SASEC,11-13 mai 2015, 254-259. http://hdl.handle.net/2263/49589.

[8] M. Lacroix, numerical simulation of a shell-and-tube latent heat thermal energy storage unit. Solar Energy, Vol. 50(4) (1993) 357-36.

[9] J. Ho et J. Y. Gao, Preparation and thermophysical properties of nanoparticle-inparaffinemulsion as phase change material, Int. Comm. in Heat and Mass Transfer, Vol.36, (2009) 467–470.

[10] J. M. Khodadadi et S. F. Hosseinizadeh, Nanoparticle-enhanced phase change materials (NEPCM) with great potential for improved thermal energy storage. Int. Com. in Heat and Mass Transfer, Vol. 34, pp. 534–543, (2007).

[11] S.Wu, D. Zhu, X. Li, H. Li, J. Lei, Thermal energy storage behavior of Al2O3 _H2O nanofluids. Thermochim Acta 483:73-77.

[12] Qinbo He, Shuangfeng Wang, Mingwei Tong etYudong Liu, Experimental study on thermophysical properties of nanofluids as phase-change material (PCM) in low temperature cool storage. Energy Conversion and Management, Vol. 64, (2012). 199–205.

[13] Trigui A., Karkri M., Boudaya Ch., Candau Y., Ibos L., Fois M. Experimental investigation of acomposite phase change material: thermal-energy storage and release. J Compos Mater 2012[reference: JCM-12-0304].

[14] M.A. Puerto, N.M. Balzaretti,Raman and infrared vibrational modes of tricosane paraffin under highpressure,Vibrational Spectroscopy, Vol. 75, (2014). 93–100.

[15] Feng Zhanga, Tian-Yu Liub, Gui-Hua Houa, Rong-Feng Guana, Jun-HaoZhangc,Preparation of paraffinpoly(styrene-co-acrylic acid) phase changenanocapsules via combined miniemulsion/emulsion polymerization,Journal of Nanoscience and Nanotechnology, Vol. 18, (2018). 4413–4417.

[16] Mohammed M. Farid, Amar M. Khudhair , Siddique Ali K. Razack , Said Al-Hallaj , A review on phase change energy storage: materials and applications, Energy Conversion and Management , Vol.45 (2004) 1597–1615.

[17] Lana Khanifah,Susilo Widodo, Widarto, Ngurah Made Dharma Putra, and Argo Satrio, Characteristics of Paraffin Shielding of Kartini Reactor, Yogyakarta, ASEAN Journal on Science & Technology for Development, Vol. 35, (2018). 195–198.

[18] Belen Zalba, Jose M Marın, Luisa F. Cabeza, Harald Mehling, Review on thermal energy storage with phasechange: materials, heat transfer analysis and applications, Applied Thermal Engineering 23 (2003) 251–283.

[19] G. Varshney, S.R. Kanel, D. Kempisty, V. Varshney, A. Agrawal, ,, E. Sahle-Demessie, R.S. Varma, M.N. Nadagouda, Nanoscale TiO2 films and their application in remediation of organic pollutants,Coordination Chemistry Reviews (2015).

[20] Bedhiaf BENRABAH, Etude des Propriétés Physico-chimiques des Couches de SnO2 Préparées par la Technique « dip-coating», thèse de doctorat, Université des Sciences et de la Technologie Mohamed Boudiaf d'Oran « USTO »,2005.

[21] Guillaume Müller. Conception, élaboration et caractérisation de matériaux de composition et de miIcro structure innovants pour les micro-piles à combustible à oxyde solide. Doctorat en Science des matériaux. Université Pierre et Marie Curie - Paris VI, 2012. Français.ffNNT : 2012PAO66530ff. fftel-00833281f.

[22] MihailSecu, Corina ElisabetaSecu, Teddy Tite and SilviuPolosan; Sol-Gel Processing of Bismuth Germanate Thin-Films; Coatings 2020, 10, 255.

[23] Elise Berrier, élaboration par voie sol-gel et étude structurale de verres de silice destinés à la fabrication de fibres microstructurées, doctorat à Université des Sciences et Technologies de Lille ;2005. http://www.theses.fr/2005LIL10118.

[24] Ecaterina Magdalena MODAN, Adriana Gabriela PLĂIAŞU, advantages and disadvantages of chemical methods in the elaboration of nanomaterials, the annals of "dunarea de jos" university of galati fascicle ix. Metallurgy and materials science No. 1 - 2020, ISSN 2668-4748; e-ISSN 2668-4756.